Molecular adsorbtion probed by the methods of Surface Resistance and Far Infrared Reflectivity

Author:

Andreas Otto

Affiliation:

Institute of Experimental Physics of condensed matter,
Heinrich-Heine-Universität
Düsseldorf, Germany

Correspondence address:

Andreas Otto
E-mail: andreasotto314@gmail.com

Abstract

The resistance of thin silver films in ultrahigh vacuum (UHV) and of thin silver- and gold electrodes changes considerably by adsorption of various molecules or halide anions in the first monolayer . This surface resistance change depends on the adsorbed molecular species, and on the energy difference between the Fermi level and the lowest unoccupied level of the adsorbate. The sensitivity for Cd ions in water is in the ppb range. The under potential deposition of Pb and Cu ions on Ag and Au electrodes is connected by very strong changes of the surface resistance. Reconstruction of Au electrodes was observed. With far infrared synchrotron radiation the predicted linear relation between surface resistance and reflectivity at grazing incidence was verified. This method allows measuring the interaction of different adsorbed species and the role of adsorbed Cs. The surface currents on Cu(110) single crystal are very different in the directions parallel and perpendicular to the Cu surface chains.

Copyright 2017 KEI Journals. All Rights Reserved

Introduction

Surface science applies many methods to explore the metal-adsorbate system, for instance low energy diffraction (LEED) to analyze the surface orientation, photoemission (PE), inverse photoemission, thermo-desorption-spectroscopy (TDS), Scanning tunneling spectroscopy (STM), near edge x-ray absorption fine structure (NEXAFS), Infrared spectroscopy, Helium scattering, adsorbates at electrodes in electrochemistry, surface enhanced Raman spectroscopy (SERS), and attenuated total reflection(ATR) – spectroscopy. This article describes the change of DC-resistance and the far infrared reflectivity of silver films by adsorption of various molecular species bound in the first layer. The measurement of surface resistance is as yet a rather unknown method of surface science.

1) Surface resistance is caused by excitations of electron hole pairs

If one adds a monolayer of silver on a silver film, the DC resistance of this film will decrease. However, adsorbing a monolayer of molecules leads to an increase of the DC-resistance of the silver film. This increase is called surface resistance. The surface resistance is caused by transient short time electron transfer from the Fermi-level to the lowest unoccupied energy level (LUMO) of the adsorbate.

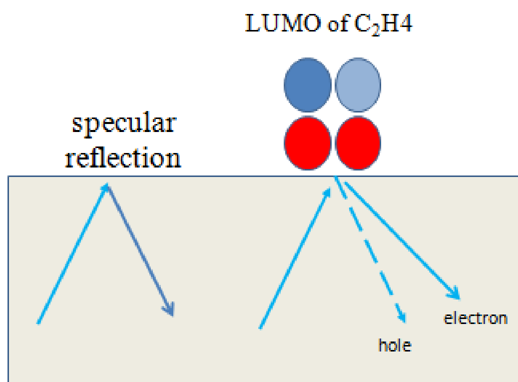

Figure 1. Reflection and scattering of metal electrons at the surface of a free electron metal

In figure 1, an ethylene molecule (C_2H_4) is weakly adsorbed at the surface of a free electron metal (for instance silver). An electron below the Fermi energy is transferred to the LUMO (lowest unoccupied molecular orbital) of C_2H_4. The energetic half-width of the LUMO is of the order of 1eV as measured by inverse photoemission. Without coverage, the electron would be specular reflected, see figure 1,left. Specular reflection does not contribute to the resistance of the silver film. However, by entering the LUMO (here, for instance ethene (ethylene), the electron will be scattered randomly in the direction of the full arrow. The electron is missing in the reflected state (dashed arrow). This state is the so-called hole. In this way, electron hole pairs are excited. This energy dissipation is observed as electrical resistance, induced by the adsorbate. Hence, it is called surface resistance. The transition will depend on the energy of the LUMO above the Fermi level and therefore the surface resistance will be “chemically specific”. The rare gas Xenon has a filled electron shell, therefore, an electron cannot enter the Xe atom and, therefore, there will be no surface resistance by adsorbed Xe, as indeed observed, see figure 7 below.

2) Experimental technology

A review of the measurement of DC resistance of thin solid films, concerning the growth mechanism, structures of thin films, metal diffusion, gas coverage and surface structure has been given by Dieter Schumacher[1] in the year 1992. He joined the institute in 1992. Without his initial technology (see figure 2) the further activities in surface resistance would have never been started. He introduced the setups in figures 2 and 3.

Copyright 2017 KEI Journals. All Rights Reserved

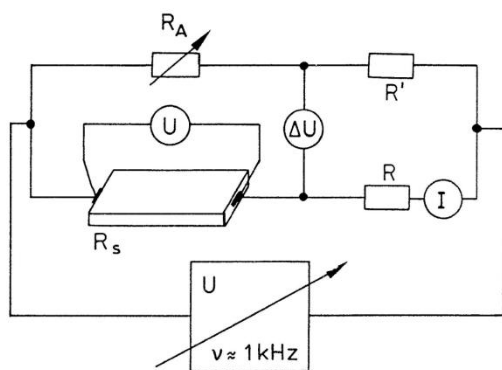

Figure 2. Wheatstone bridge for measuring the bulk resistance R_s of a thin metal film.

In figure 2, the resistors R and R' are much higher than R_s and R_A. The voltage meters U and ΔU have high input resistance. The current I is constant for changes of R_s in a limited range. Therefore, the voltages U and ΔU are directly proportional to R and ΔR. The circuit is supplied with an alternate voltage source U because it is technically easier to detect small AC than DC voltages. The AC current is about 5 A/mm^2 [1].

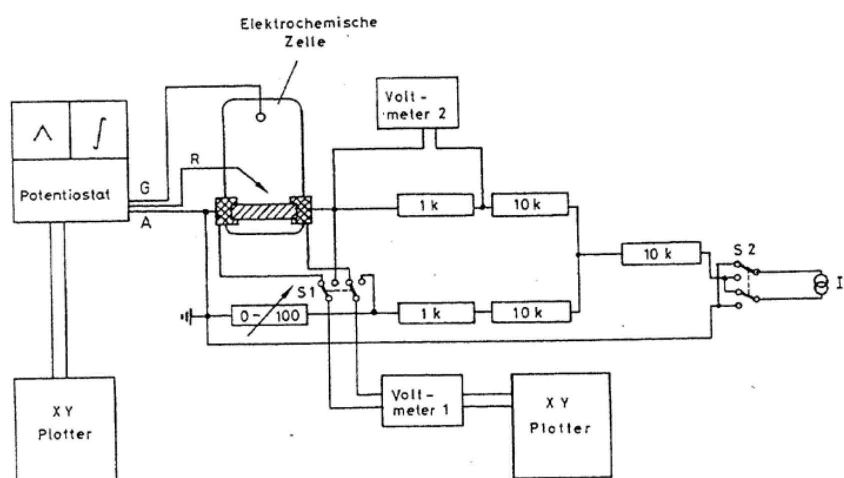

Figure 3. Setup of the resistance measurement of thin film electrodes in aqueous electrolyte. A: connection to the thin Ag film anode (working –electrode), R: reference-electrode, C: counter-electrode. The working-electrode consisted of a silver film of 20-30 nm thickness with 100 nm contacts.

In figure 3, the switch S1 connects to the potentiostat or to the Wheatstone bridge. Switch S2 changes the direction of the current through the silver film. With voltmeter 1, the resistance R, and after calibrating the bridge, the change of resistance ΔR could be measured, respectively. The potentiostat delivers electrode potentials with anodic and cathodic sweeps (left sign on top of the potentiostat) and Coulometer (right sign of the potentiostat) which integrates the current between Counter electrode G and working electrode[2]. These electrochemical expressions are explained in chapter 5.

Copyright 2017 KEI Journals. All Rights Reserved

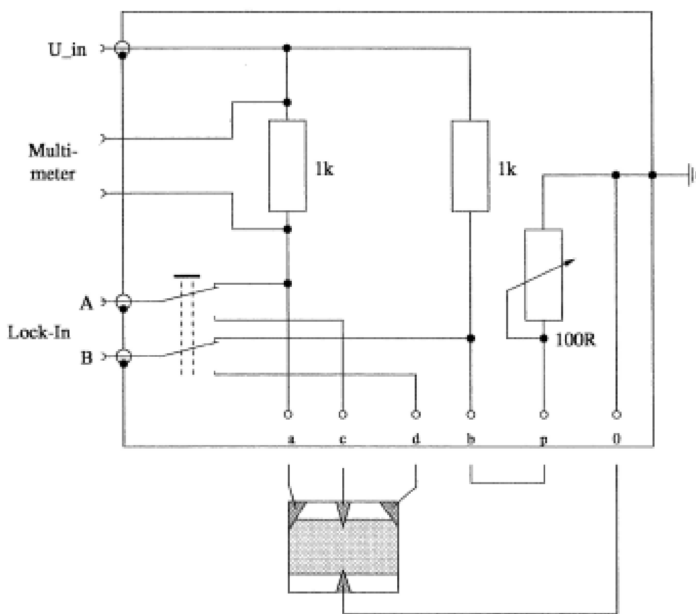

Figure 4. Circuit diagram for the measurement of the sheet resistance of thin silver films in Ultra High Vacuum (UHV).

The switch in Figure 4 allows changing between the 4-point measurement and the two-point method. The voltage is provided by a Lock-in Amplifier. The bridge b and p was not used. The 4-point method uses separate pairs of current-carrying and voltage-sensing electrodes to make more accurate measurements than the simpler and more usual two-terminal sensing. [3].

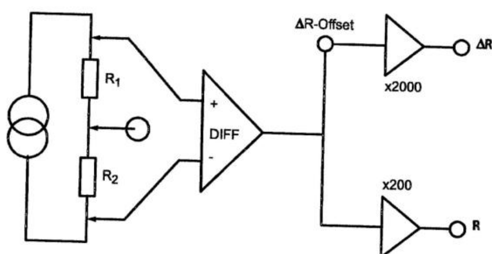

Figure 5. Scheme of the circuit diagram of an instrument build at the Institute of electrochemistry at the University of Düsseldorf[4].

3) Sample preparation

During the evaporation process, a number of defects are incorporated into the metal film, and annealing is necessary to obtain films with a maximum conductivity. The DC resistivity of a metal film is under suitable conditions a sensitive indicator of the defect density in the bulk and at the boundaries. Therefore, the in situ thermal treatment was monitored by continuously measuring the film resistance R .The films are heated with a rate of about r = 0.5 K/s to the annealing temperature-T_A, see figure 6.

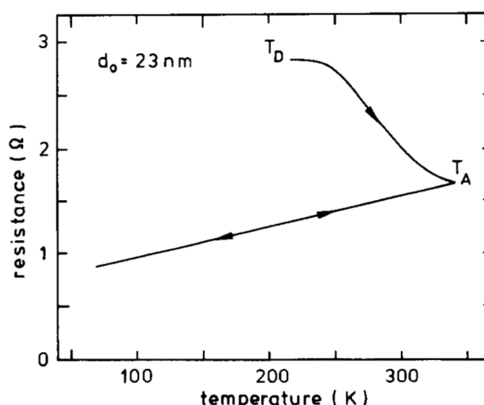

Figure 6. Irreversible and reversible temperature dependence on the film resistance of a silver film of 23 nm thickness, deposited at T_o = 225 K and annealed to T_A = 340 K. [5]

Usually, the silver films were deposited at room temperature on various substrates.

4) Theory

The resistance of a thin smooth silver film R increases by adsorption of a monolayer of molecules by ΔR. ΔR does not depend on the thickness of the silver film nor on the adsorption of multilayer's of molecules, see Figure 6a. Delta ΔR is the surface resistance.

From the initial slope of the resistance increase versus coverage , one can obtain the

Copyright 2017 KEI Journals. All Rights Reserved

cross section "diffuse" scattering of conduction electrons from the first film surface with the help of the definition[6]

$$\Sigma = \frac{16}{3}\frac{ne^2 d}{mv_F}\frac{\Delta R}{n_a} \quad (1)$$

and the damping rate of the vibration [6]

$$\frac{1}{\tau} = \frac{16}{3}\frac{ne^2 d}{mv_F}\frac{\Delta R}{n_a} \quad (2)$$

In equations (1) and (2), d is the thickness of the film, m the electron mass, n is the electron density in the films, v_F is the Fermi-velocity, n_a the surface density of the adsorbed molecules and ΔR is the surface resistance.

5) Surface resistance measurements in ultra high vacuum (UHV)

Fig. 7 (right) Thermo desorption spectra of C_HB adsorbed on smooth silver film exposed to 1 and 1.5 L of C_2H_6, with heating rate of about $1.5Ks^{-1}$, measured with a quadrupole mass spectrometer (QMS) [7].

The annealing of the silver films at 350K guarantees smooth silver films of (111) orientation. The exposure of 1 L (Langmuir) corresponds approximately to the formation of one monolayer at sticking coefficient 1. In any case, multilayers desorb at higher temperatures than the first layer. An example is shown in figure 6 for C_2H_6. The first monolayer desorbs at 100K, the additional adsorbed layers desorb at 76K. For the 5 kinds of adsorbates, the relative resistance change $\frac{\Delta R}{R}$ becomes constant above an exposure of about $1x10^{15}$ molecules per cm^2. This corresponds to the formation of the first monolayer. The growth of further layers does not change the resistance, as expected. However, the saturation values of R depend strongly on the adsorbate. ΔR is the surface resistance.

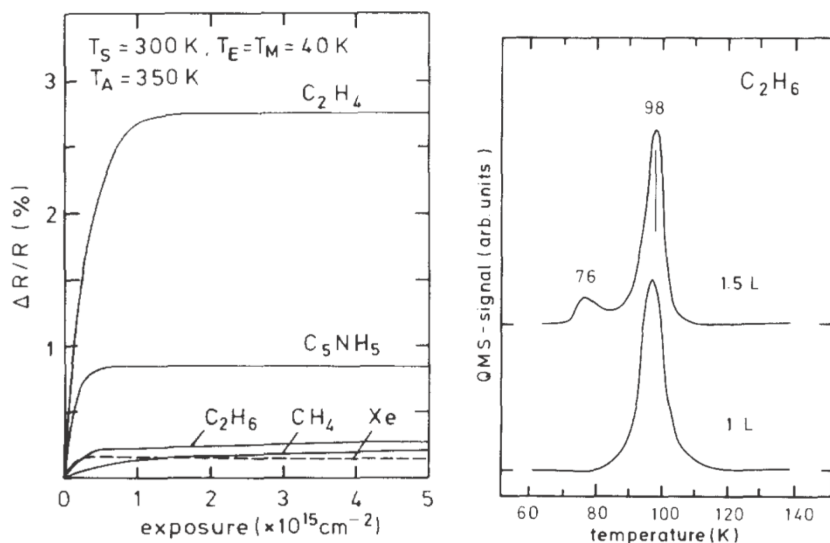

Figure 7. (left): Resistance R and resistance variation ΔR of silver films, deposited at 300K in ultrahigh vacuum (UHV), annealed at 350K and cooled to 40K, and measured at 40K during exposure with CH_4 , C_2H_4, C_2H_6, C_5NH_5 and Xe. The resistance R at 40K before exposure was 0.35, 0.32, 0.31, 0.30 and 0.77 Ohm respectively [7].

Copyright 2017 KEI Journals. All Rights Reserved

The surface resistance ΔR can be explained by transient electron transfer from the silver surface to the first layer of adsorbates. The noble gas Xe has a filled electron shell, and does not accept electrons. Methane CH_4 and ethane C_2H_6 have no empty π^* states, only σ^* states at higher energy and hence there is little transient electron transfer from the Fermi level E_F of silver to the σ^* states. However the pyridine π^* state of pyridine adsorbed on the Ag(111) surface is only 3 eV above the Fermi energy E_F , as measured by inverse electron spectroscopy [8]. For ethene C_2H_4, the π^* level is probably closer to E_F and hence $\frac{\Delta R}{R}$ is larger in comparison to pyridine. We missed to measure ΔR for CO.

6) Surface resistance of samples in electrolytes

In the following, the surface resistance of thin silver film anodes is measured in aqueous electrolytes by shifting the Fermi level with respect to the reference electrode SCE (saturated calomel electrode). The current of anions and cations (see figure 8) within the electrolyte is flowing between working electrode and counter electrode, see figure 8.

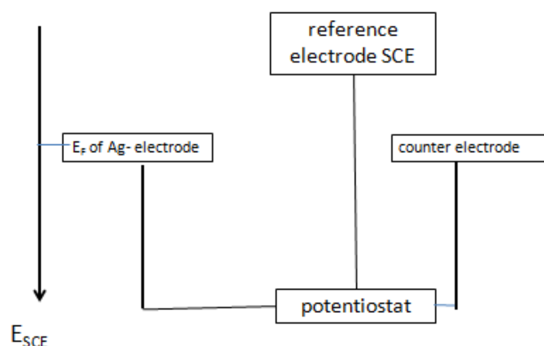

Figure 8. The regulation of the potential E_{SCE} of a silver working electrode with respect to the non polarisable saturated calomel reference electrode (SCE) . E_F is the Fermi energy of the silver electrode.

The current between the counter electrode and the working anode is given by the drift on anions or cations to the working silver electrode. There is no change of the potential within the electrolyte. The potential changes are given by varying the concentration of ions in front of the metal. The conventual model of the electrochemist is displayed in figure 9.

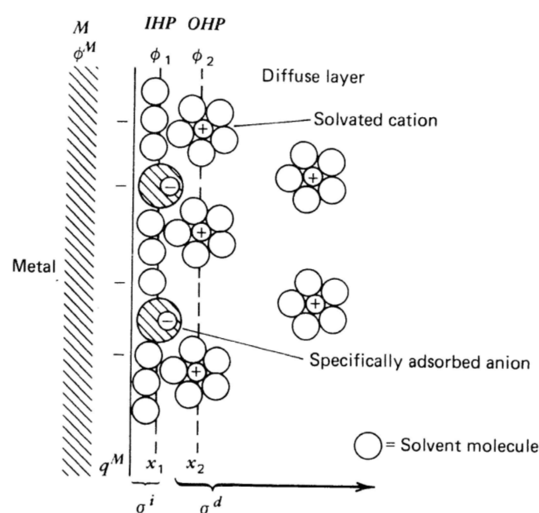

Figure 9. Proposed model of the electrode-solution, double layer region, at a negatively charged metal working electrode M[9]. IHP: Inner Helmholtz plane, OHP: Outer Helmholtz-plane. σ_i is the ionic charge in the inner Helmholtz layer, σ_d the sum of the charges in the second layer and the diffuse (or Gouy-Chapman) layer. Φ^M, Φ_1, Φ_2 are the electrostatic potentials of the metal electrode, the inner and outer Helmholtz planes.

Specifically adsorbed anions are for instance Cl^-, nonspecific adsorbed ions are for instance ClO_4^- and $(PF_6)^-$, a specifically adsorbed cation is for instance Cd^{2+} (see chapter 6). An example of measuring the surface resistance of thin film electrodes is displayed in figures 10a and 10b.

Copyright 2017 KEI Journals. All Rights Reserved

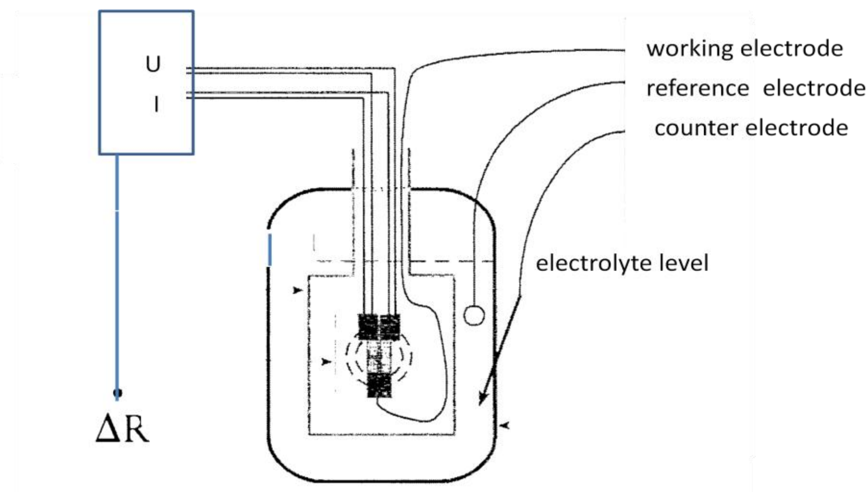

Figure 10 a). Measuring the surface resistance with the 3 contact method [10]

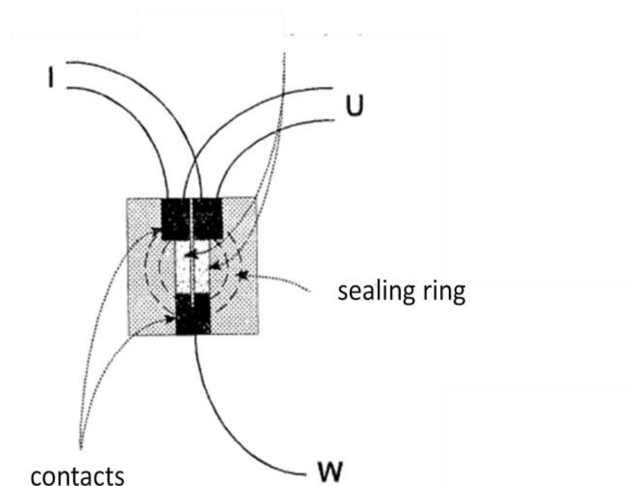

Figure 10 b). Counter-current method [10] W: Working electrode. The sealing ring and a plate on top keeps the electrolyte above the sample.

The working electrode W in Fig 10b consists of 2 parallel silver films, with 3 contacts. This is very helpful, because the 2 currents from the counter electrode to the 2-film electrode are not changed by the current from the counter electrode to the 2-film sample. When this current increases on the left side, it increases on the right side, but the sum of the currents remains constant. Therefore, there is no influence on the surface resistance by the current from the counter electrode through the electrolyte to the working electrode[10].

The resistance change by the non-specifically adsorbed anion PF_6^- is very small, (less than 0.12%) see in Fig. 11[4].

Copyright 2017 KEI Journals. All Rights Reserved

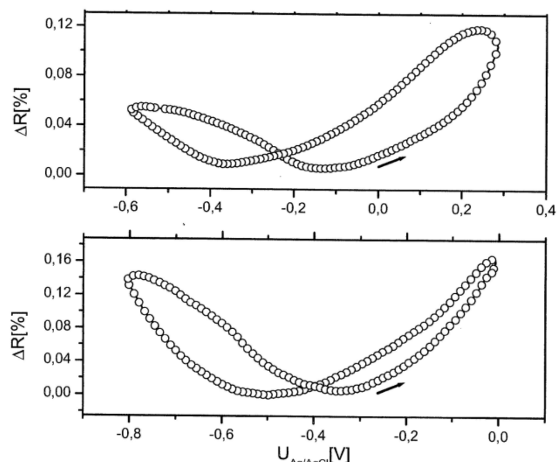

Figure 11. Resistance in % of a 40nm thick Ag(100) film (above) and a 40nm thick Au(111) film (below) in 10mM KPF_0 aqueous electrolyte. Sweep directions are indicated [4].

The surface resistance change in figure 11 of about 0.1% is much smaller than in halide-electrolytes in Fig. 12 (note the different ΔR scales in figures 11 and 12).

In the following experimental results, the surface resistance depends on the surface coverage of specifically adsorbed anions (e.g. Cl^-, Br^-, J^-). [10]

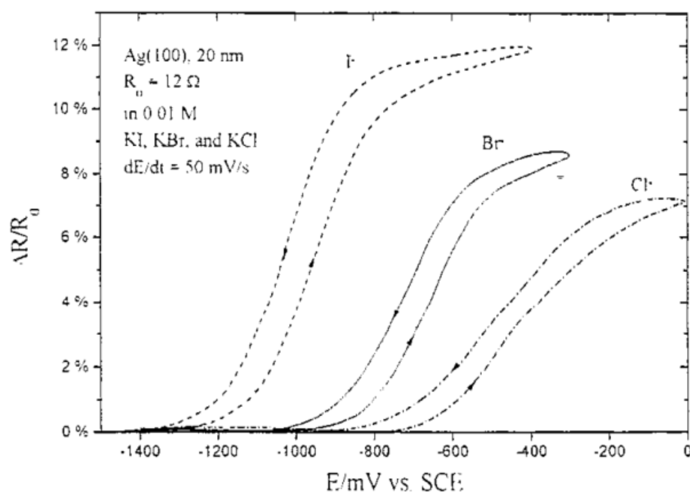

Figure 12. Comparison of the relative resistance change ΔR of a 20nm Ag(100) thin film electrode grown on a smooth Mg(100) substrate, as function of the electrode potential E.

Figure 12 shows the increase of the resistance caused by the adsorption of the halide anions Cl^-, Br and I^- see Fig. 8) and desorption (decrease of R) of the anions (see Fig. 8) The electrolytes were 0.01M KCl, 0.01M KBr and 0.01M KJ. The minimum of the absolute resistance was 12 Ohm in all cases. The scan rate was 50mV s^{-1}. The directions of the scans are indicated, the upper scan for increasing potential E, the lower scan for decreasing potential E. [10].

The results in Fig. 12 may be explained in the following qualitative way: When the potential E_{SCE} of the Ag(100) electrode become less negative, the surface concentration of Cl^-, Br^- and I^- at the silver (100) film increases because the Coulomb repulsion between these anions and the negatively charged silver surface decreases. Coulomb repulsion becomes less, when the radius of the anions increases. These radii are shown in Fig. 13.

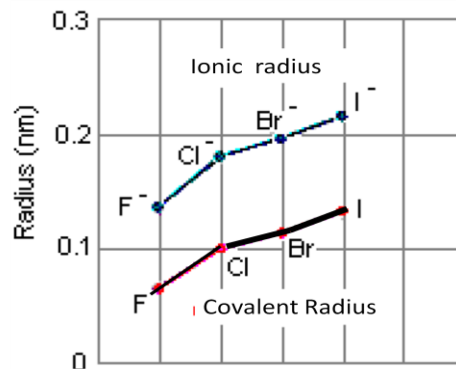

Figure 13. Covalent and ionic radii obtained from http://www.science-at-home.de/wiki/index.php/Radien

In Fig. 12, the sweep up to higher resistance is the right line, the sweep to lower resistance the left line. The hysteresis visible in Fig. 12 increases with the scan rate, as shown in Fig. 14.[11].

Copyright 2017 KEI Journals. All Rights Reserved

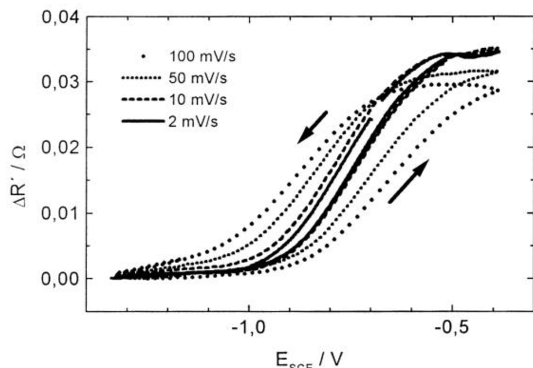

Figure 14. Potential controlled change ΔR of the resistance R of a 20nm thick Ag(100) film in 0.04M $KClO_4$ and 0.01MKBr for different scan rates as indicated. The epitaxial Ag(100) film was grown on MgO (100).[11].

The hysteresis at low sweep velocities in Fig. 12 may be influenced by stripping or creation of the hydration shell of the anions. Hydrated anions have less Coulomb interaction with the silver anode, therefore they are less bound and need less repulsion from the silver surface in order to desorb. In summary, one understands qualitatively the differences between the different ions and the hysteresis in Fig. 12.

Figure 14 shows the change of resistance of 25nm thick silver films with (111) orientation grown on Si(111).

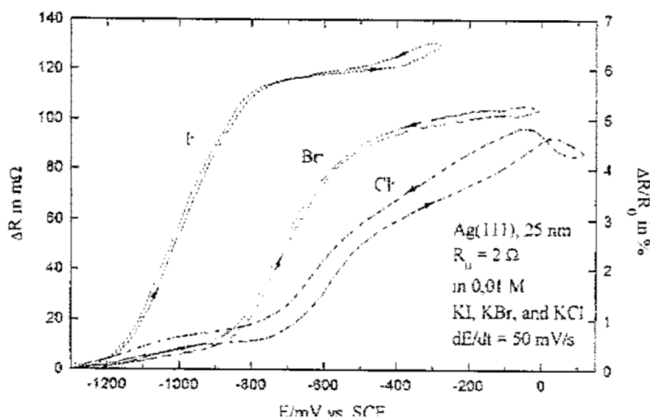

Figure 15. Comparison or the absolute resistance change ΔR ($m\Omega$) (left scale) and the relative resistance change $\Delta R / R_0$ (right scale) of a 25nm Ag(111) thin film electrode on Si(111). The electrolytes were 0.01M KCl, 0,01 M KBr and 0,01M KJ. The minimum of resistance was 2 Ω in all cases [10]

In Fig. 15 the resistance curves show a superimposed slope because of the Si (111) substrate has a non-vanishing conductance. One observes a similar influence of the adsorbed halides on the surface resistance of the Ag(111) thin film electrode as seen in in the case of the Ag(100) surface in figure 12. [12]. The decrease of ΔR for E >0 is assigned to the formation of an ordered $\sqrt{3} \times \sqrt{3} R30^0$ surface layer of Cl^- [12].

8) Detecting small concentration of metal cations in water[13].

For the electrode preparation, the process steps of silicon planar technology were employed. Commercially available silicon wafers with an <100>-surface orientation and a resistivity of 2±100 kΩ served as substrates for the thin film electrodes which were deposited by electron-beam evaporation under high vacuum conditions. The thin film electrodes consist of a 5-nm thick polycrystalline chromium layer and a 15-nm thick polycrystalline gold film. The chromium layer serves as an adhesion promoter between the Si/SiO_2 substrate and the gold film. Patterning of the metal structures was achieved by optical lithography. The large resistivity of the wafer and a natural oxide on its surface make parasitic currents through the substrate negligible. Via 200-nm thick conducting tracks, which were also realized by the described procedure, current and voltage are supplied to the electrodes. Except for the thin film electrodes and the bond pads, which are needed for the electrical connection, the wafer was covered by a 1 mm thick electrically insulating polyimide.

Copyright 2017 KEI Journals. All Rights Reserved

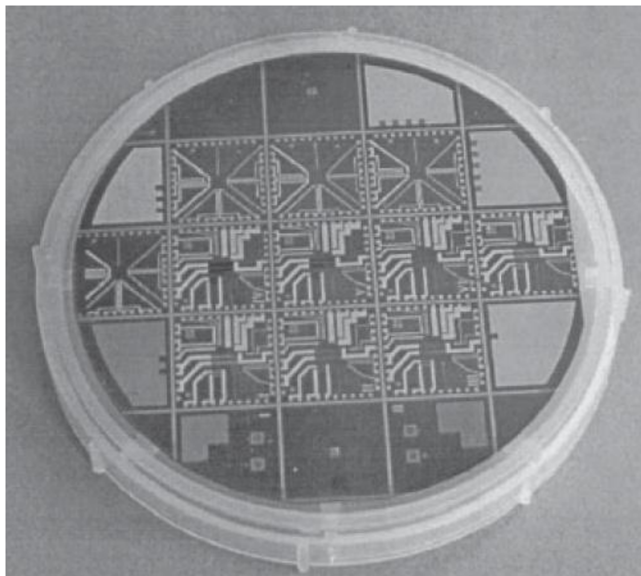

Figure 16. Photograph of a processed 3-inch silicon wafer with 7 micro- structured electrodes [13]

The thin film electrodes consist of a 5-nm thick polycrystalline chromium layer and a 15-nm thick polycrystalline gold film electrode. The chromium layer serves as an adhesion promoter between the Si/SiO_2 and a 15 nm thick polycrystalline gold film see Fig. 16 [13].

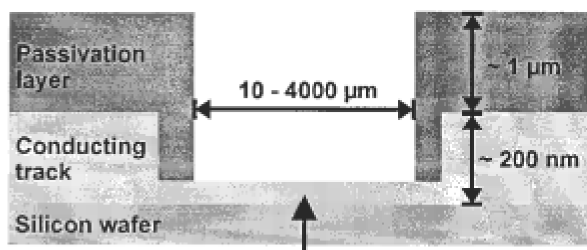

Figure 16. Cross-sectional scheme of the realized thin conducting Au-film structure. [13]

Each electrode consists of two identical parts which are connected in series by a metallic pad that serves also as the connection of the electrode to the potentiostat. This arrangement ensures that electrochemical currents do not influence the resistance measurements as discussed with the help of figure 16. All chemicals used were of analytical grade and bi-distilled water was used for dilution. Working standard solutions of different concentrations of Cd,Pb,Ni,Tl and Zn cations were prepared from 1000 mg/l stock solutions.

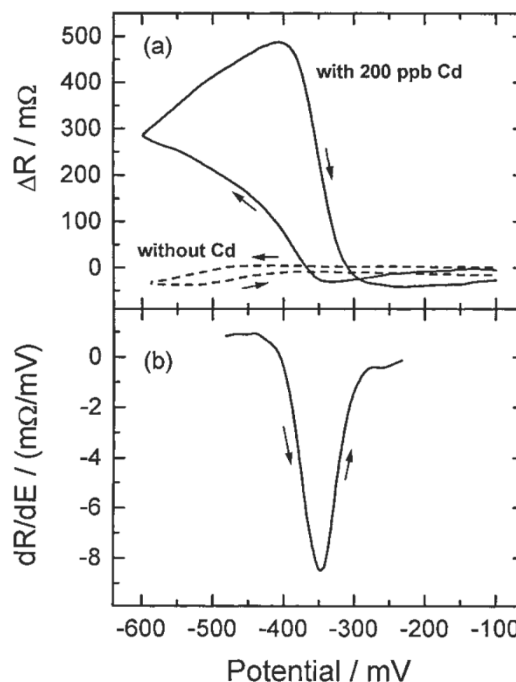

Figure 17. a). Cyclic surface resistance measurements in a heavy metal free solution (dashed curve) and a Cd^{2+} containing electrolyte (200 ppb) and b) its derivative dR/dE in the range of decreasing electrode potential E of the electrode (see Fig. 8). **(b)** Derivative in the potential range of Cd desorbing as Cd^{2+} [13].

In the cathodic sweep in fig 17a (Potential of the electrode becomes more negative), the Cd^{2+} is adsorbed as neutral Cd on the silver electrode, increasing the surface resistance. Though the potential sweep is reversed, the neutral Cd coverage still keeps growing up to a potential of the electrode about -400mV. This is supported by the stripping results in Fig. 18.

Copyright 2017 KEI Journals. All Rights Reserved

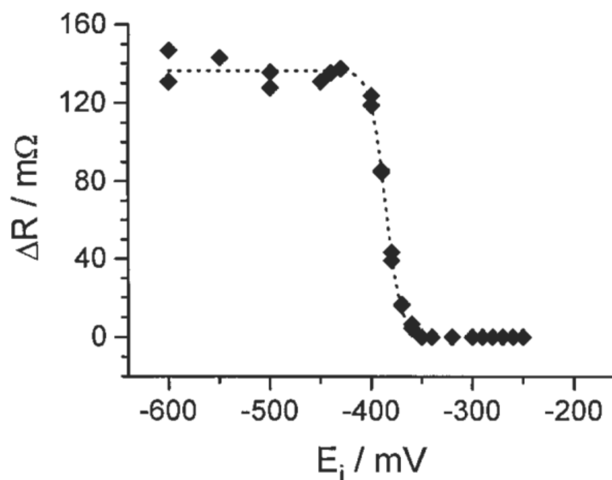

Figure 18. Resistance changes during stripping experiments in a Cd^{2+} -containing solution as function of the deposition potential E_i. [13].

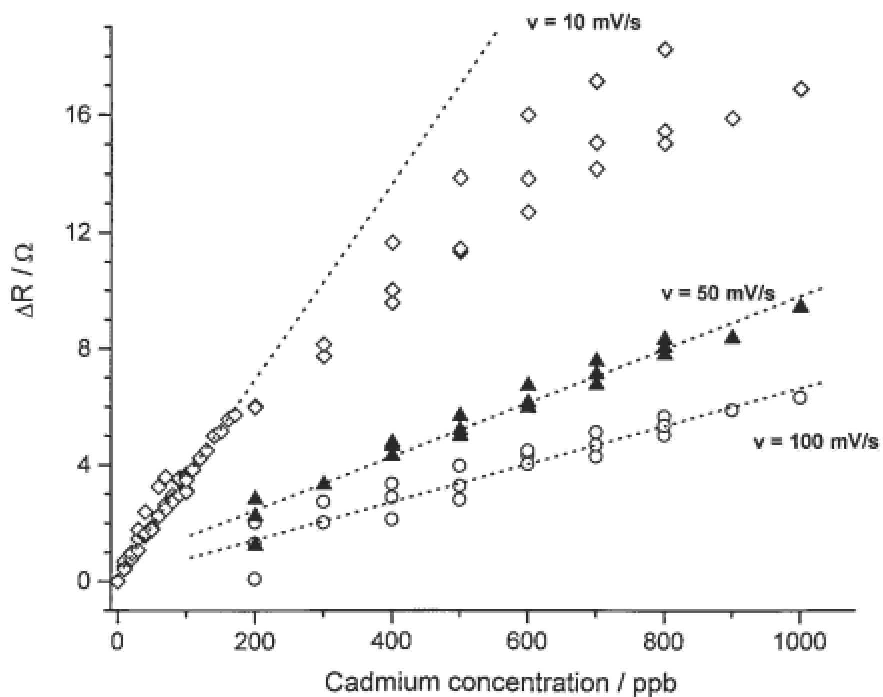

Figure 19). Increase of the measured resistance change ΔR for various cadmium anion concentration and scan speeds [13]

Copyright 2017 KEI Journals. All Rights Reserved

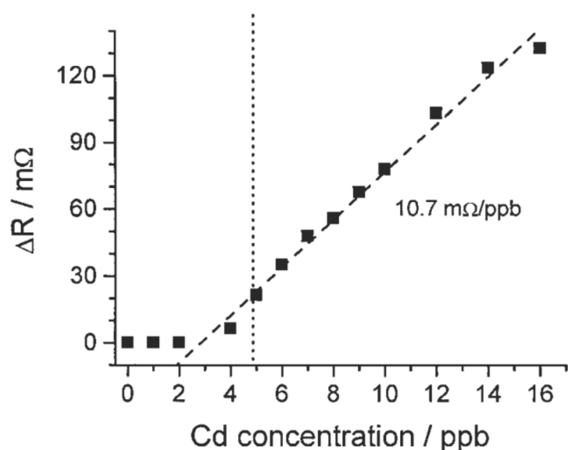

Figure 20. Resistance changes during cyclic measurements at ppb concentrations of cadmium ions. The recommendation of the world health organisation WHO for the maximum cadmium content in drinking water is indicated by the dotted line at 5 ppb.[13]

9) Surface oxydation and reduction of a Au film

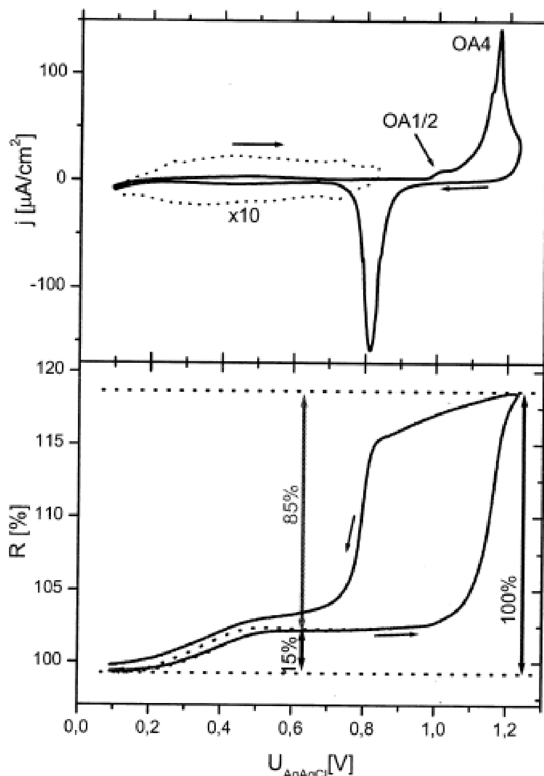

Figure 21. Cyclovoltamogram j(U) (above) and resistance R during oxydation of Au (111) surface creating Au^+ ions in the electrolyte (→) and reduction of Au^+ and redeposition of Au^+ gold on the Au (111) layer <--- with thickness of 30nm in an 0.1 M H_2SO_4 . The cyclovoltamogram in the double layer range between 0.2 and 0.8 V is given by the dotted cycle. [4]

In Fig. 21, the shoulder OA1/2 is assigned to the oxidation Ag→Ag^+ at atomic steps, the structure OA_4 to the oxydation of full monoatomic layers (terraces), leading to further atomic scale roughening. The resistance R increases strongly when full terraces are oxidized, leading to further monolayer steps. In the cathodic sweep (decreasing U), the surface resistance decreases only when the newly created atomic scale roughness is annealed. This field has been studied intensively by scanning tunneling spectroscopy [14].

10) Resistance of thin Ag- and Au film electrodes during under-potential deposition and desorbtion of Cu and Pb [4].

Under-deposition signifies that in a cathodic sweep of a gold electrode in an aqueous electrolyte containing Cu^{2+} ions (from dissolved Cu_2SO_4) or Pb^{2+} ions (from dissolved Pb_2 SO_4) the first layer of neutral Cu or Pb or is deposited at a less cathodic potential than thicker layers of Cu or Pb. By various surface science methods the surface structure it was found that Cu overlayer on Au(111) has a $Au(111)-(\sqrt{3}\times\sqrt{3})R30°$ structure, see Figure 21 [15].

Copyright 2017 KEI Journals. All Rights Reserved

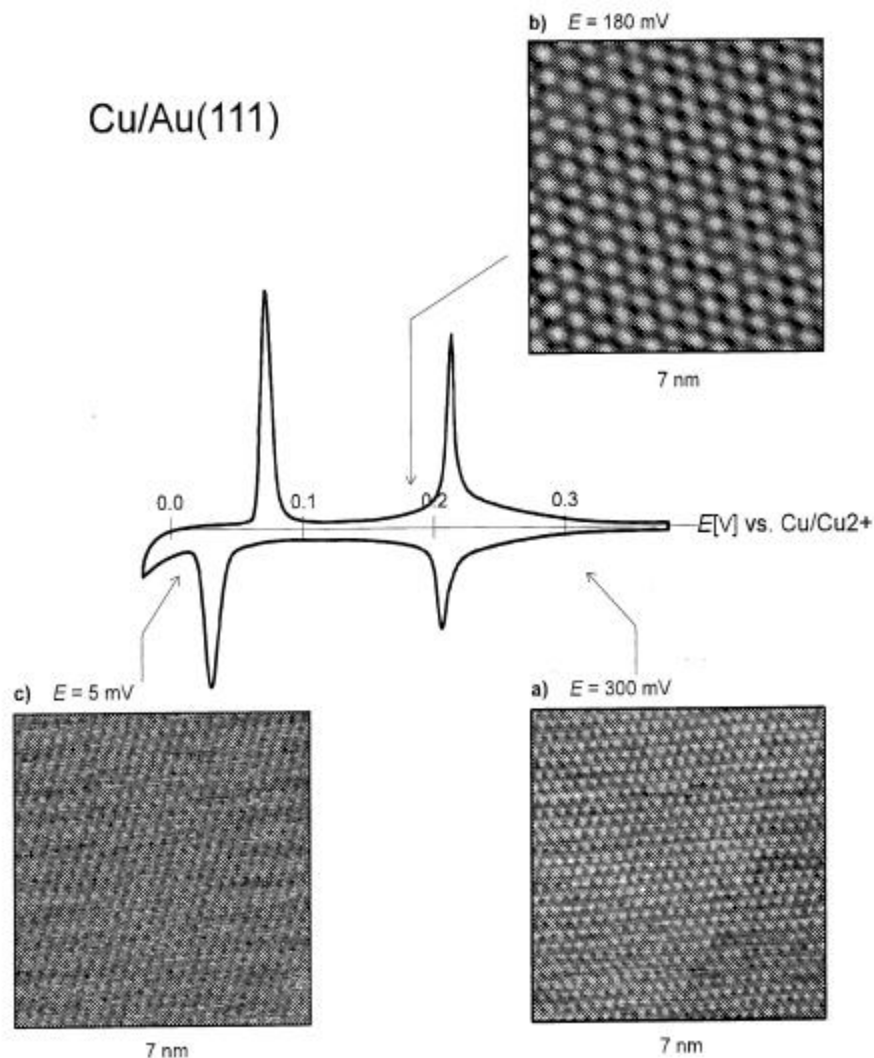

Figure 22. a) Cylovoltammogram and STM images of the system Au(111) in 10^{-3}M $CuSO_4$ in situ. The sweep direction towards smaller [E(V)] yields the current below zero. The onset of Cu multilayer growth is at E[V] =0 The atomic structures are obtained by in situ Scanning Tunneling Microscopy. [15].

The resistance Delta R and the voltammogram of an Au (111) film have been measured simultaneously, see Fig. 22.

Copyright 2017 KEI Journals. All Rights Reserved

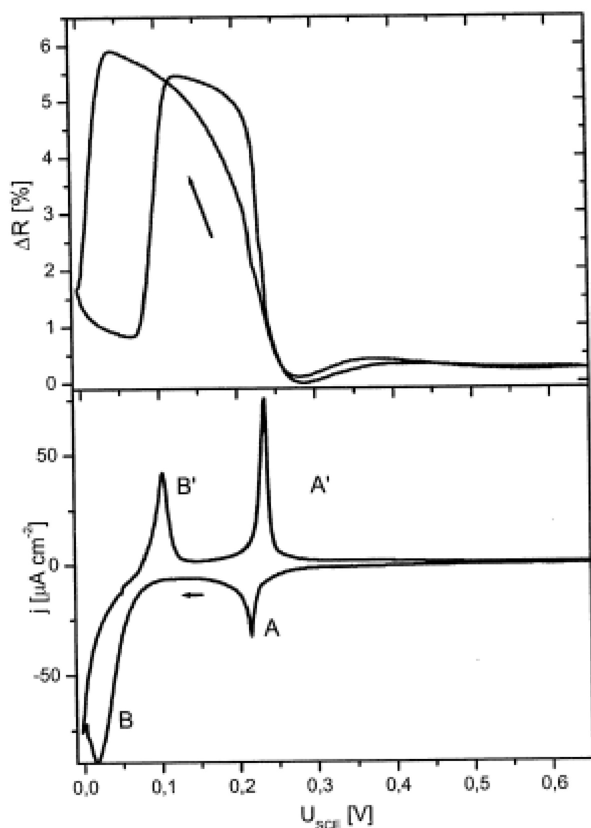

Figure 23. Voltammogram and resistance of 30nm thick Au (111) film in an electrolyte (1mM $CuSO_4$ +50mM H_2SO_4) and scan velocity 5 mv/s [4].

The voltammogram in Figure 22 resembles that in Figure 21. The resistance shows a strong increase at the copper adsorption peak A. It keeps growing up to the electrode potential U_{SCE}= 0.05 V where bulk deposition of Cu starts. This leads to a strong decrease of the resistance. Reversing the sweep to higher electrode potentials USC yields again a strong increase of resistance because the thick Cu film shrinks to about a monolayer. In this monolayer range the underpotential film structures (Fig. 21) appear again. Only when these surface reconstructions induced by Cu^{+1} ions disappear, the surface resistance decreases and reaches the very low level of the Au(111) film electrode again .

The underpotential deposition of lead was also observed for Ag(111) films and polycrystalline Ag films.[4] The voltammogram of a Ag(100) film is more structured that that from a polycrystalline film, see Figure 24.

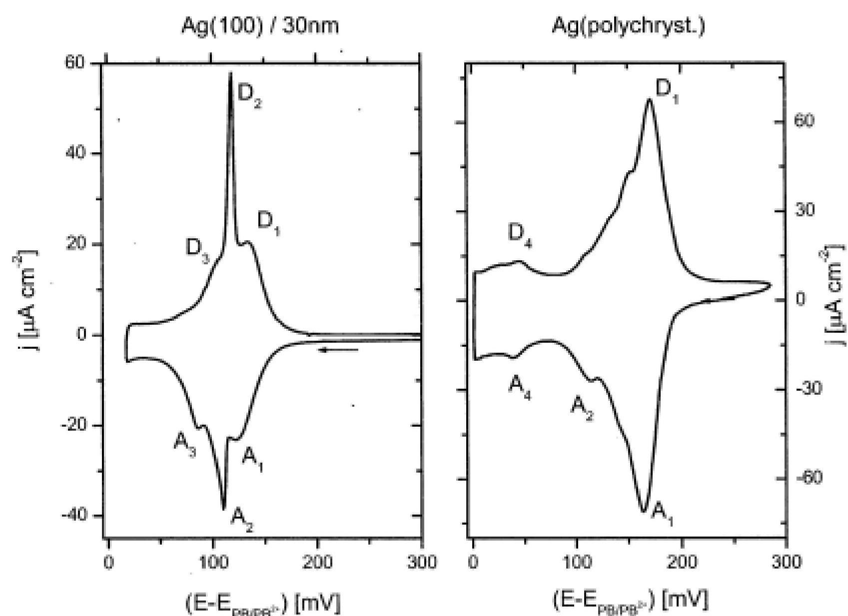

Figure 24. Voltammograms of a 30nm Ag(100) film(left) and a polycrystalline thick Ag sample (right) in the electrolyte $5x10^{-2}$ M $PbSO_4$ +5x-10^{-1}M $NaClO_4$ +$5x10^{-3}$ M $HCl0_4$. dE/dt= 10mV/s [4].

Copyright 2017 KEI Journals. All Rights Reserved

As expected the voltammogram of the Ag(100) film shows more structure than that of the polycrystalline sample.

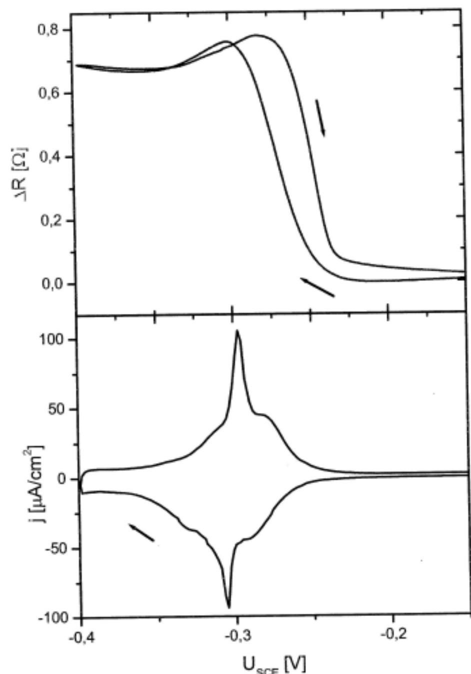

Figure 25. Surface resistance and voltammogram of the 30nm Ag(100) film in the same electrolyte as in Fig. 24 [4].

The resistance cycles for Pb UPD on Ag(100) and Cu UPD on Au(111) are similar.

11) Surface resistance and reflectance measurements at far infrared alternating currents

These measurements were performed using infrared radiations of the IR beamline U4IR (supervisor G. P. Williams) of the National Synchrotron Light Source, Brookhaven National Laboratory, Upton, NY USA, see Fig. 26.

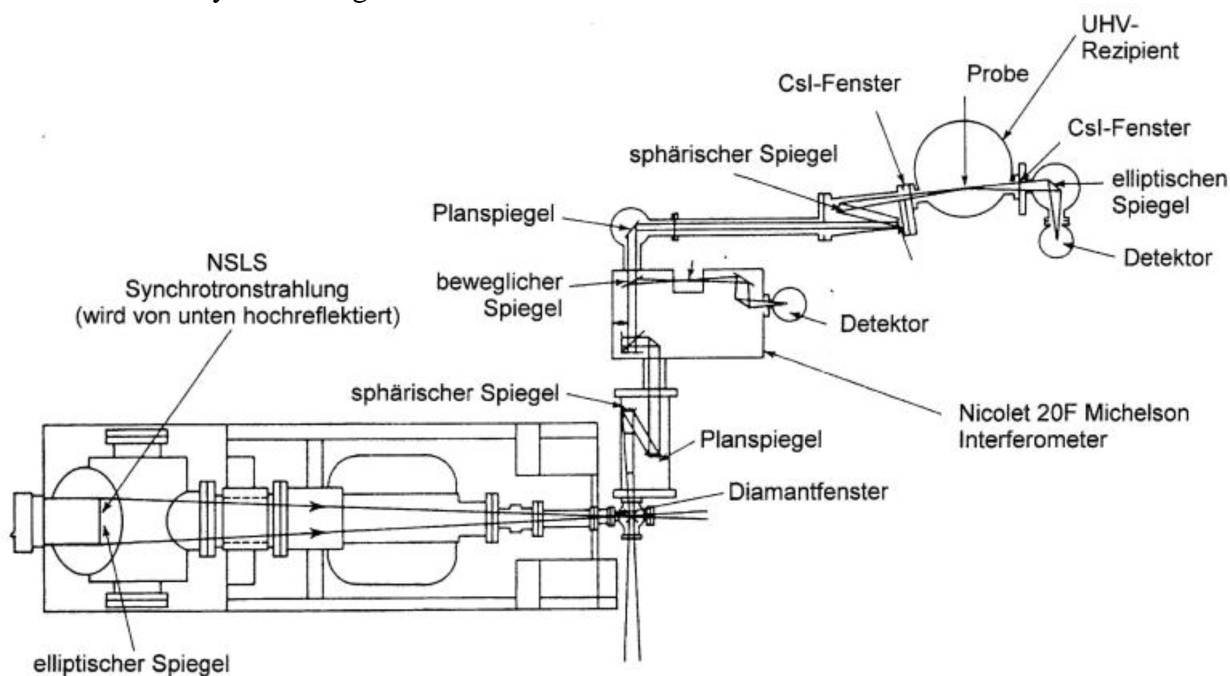

Figure 26. Radiation in the beam line U4 is deflected from ground floor to the first floor U4IR by an elliptical mirror. The high vacuum in the beam line is separated from the UHV by a diamond window. Michelson interferometer is scanning the frequency (given in cm^{-1}), both the incident

Copyright 2017 KEI Journals. All Rights Reserved

and reflected beams pass through CsI windows of the ultra high vacuum vessel. The sample holder is cooled to allow adsorption, by regulating needle valves. Detectors were a Boron-doped Si bolometer for the wavenumber range between 180-500 cm^{-1} and a Cu doted Germanium photoresistor the range of 350-to 3000 cm^{-1}. Probe = sample, Beweglicher Spiegel= movable mirror, Fenster= window.

It is worth noting that accurate measurements of the broadband IR-reflectance change are far more demanding experimentally than the more common recording of the vibrational spectrum. The main requirements are the high stability of the electron beam position in the storage ring and the high brightness of the infrared source. This intensity decreases slowly with time caused by loss of electrons in the storage ring. All spectra are normalized in respect to the electron current in the storage ring. With a thermal source, temperature fluctuations can provide uncertainty in the incident beam intensity. On the other hand, synchrotron radiation is an absolute source whose brightness, for a given ring, is determined only by the stored current which can be accurately measured. A global feedback was developed at the National Synchrotron Light Source.

The broadband IR reflectance and resistance change were acquired simultaneously for Cu (111) films, of various thickness, epitaxial grown on a TiO_2 (110) substrate. The substrate was first annealed by resistive heating for 5 hours at 973K.

Various copper film thicknesses ranging between 20 to 100 nm were made using slow evaporation rates of about 0.1nm/s. After preparation of the 15mm × 10mm film, four 200nm thick copper pads were evaporated onto the edge of the film (see Fig. 3) to allow measurement of the film resistance W. Accurate measurements of the broadband IR-reflectance change are far more demanding than the more common recording of the vibrational spectrum. The main requirements are the high stability of the electron beam position and the high brightness of the infrared source. With a thermal source temperature fluctuations can provide uncertainty in the incident beam intensity. On the other hand, synchrotron radiation is an absolute source, whose brightness, for a given ring, is determined only by the stored current which can be accurately measured. A global feedback allowed normalisation of the spectra was developed at the National Synchrotron Light Source.

The polarisation of the IR beam at frequency is p-polarized (electric vector is in the plane of incidence) and the angle of incidence is about 89°, which means at grazing incidence. Naively, one would believe that in this case the electric vector is perpendicular to the sample surface and hence the surface current is negligible. However, the exact EM calculation yields of the current within the skin depth is proportional to $\frac{1}{\cos\theta}$. The singularity at $\theta=90°$ of the current parallel to the surface is only prevented by the small factor $F=\frac{\cos\theta}{(\cos\theta)^2+\omega_p^2)}$ (3). ω_p is the plasmon frequency of Cu.

At first, only the reflectance was measured with the equipment shown in Fig. 20 , the focus was on the excitation of the normal and tangential vibration of CO adsorbed on Cu(111) films.[16] The simultaneous measurement of both reflectance and surface resistance was introduced by Hein and Otto.[3] A copper (111) film was connected as shown in Fig. 3, allowing the simultaneous measurement of

Copyright 2017 KEI Journals. All Rights Reserved

reflectivity. This predicts a linear relation between the change of reflectivity ΔR and the change of the resistance W.

Person introduced the equivalence of "friction" and "surface resistance", see Fig. 26.

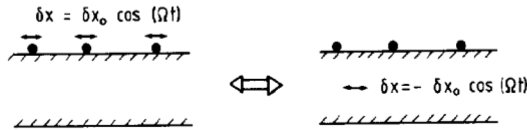

Figure 27. Equivalence of the periodic tangential motion of adsorbed molecules on a metal film ("friction", left), and "surface resistance" (right) of an AC electronic current by adsorbed molecules

The "friction" f between the adsorbate (velocity du/dot) and the free Drudge-electrons in the metal is assumed to depend only on the parallel "frustrated" drift motion of electrons right below the metal surface.[16-17] "Friction" and "Surface resistance" are equivalent expressions.

$$f=-\eta(\frac{du}{dt}-v_{pl}) \quad (4)$$

η is the electronic friction coefficient , v_{pl} is the "hydrodynamic drift velocity" right below the surface.

The change ΔW of the resistance of a thin film of thickness d, covered with n_a molecules per cm^2 is independent of the initial resistance W of the film according to Mathissen's rule and is given by

$$\Delta W = n_a \frac{M\eta}{(ned)} \times \frac{1}{(ned)}$$ where n_a is the free electron density (5)

and $$\Delta R_p = \frac{4}{c}\frac{n_a}{n}\frac{M}{m}\frac{\eta F}{\cos\Theta} \quad (6)$$

In the following, we use the cross section defined by

$$\Sigma = \frac{16ne^2d^2}{3mv_F}\frac{\Delta W}{n_a} = \frac{16M\eta}{3nmv_F} \quad (7)$$

These cross-sections range in the order of 0.1 (Angström)^2 for C_2H_6 on Ag to 13.6 (Angström)^2 for an Ag adatom on Ag [17].

The change of the broad band infrared reflectance R_p of p-polarized light in the range of validity of local optics , provided that the mean free path of the electrons is not larger than the classical skin depth , is given by

$$\Delta R_p = \frac{4}{c}\frac{n_a}{n}\frac{M}{m}\frac{\eta F}{\cos\Theta} \quad (8)$$

where m is the free electron mass, Θ is the angle of incidence and F is given by

$$F = \frac{\cos\Theta}{(\cos^2\Theta + \omega^2/\omega_p^2)} \quad (9)$$

The theory of the scattering of the conduction electrons by the adsorbate predicts a linear relation between change of the reflectivity ΔR and the change of resistance ΔW .

The ratio between the change of reflectance and the change of resistance is given by

$$\frac{\Delta R_p}{\Delta W} = \frac{\omega_p^2 d^2}{\pi c}\frac{F}{\cos\Theta} \quad (10)$$

The aim of the experiments was to measure the change of resistance ΔW with the electric circuit in figure 3 and the change of reflectance ΔR_p simultaneously. The samples were Cu(111) films epitaxial grown on TiO_2 .

The results are shown in Figure 28.

Copyright 2017 KEI Journals. All Rights Reserved

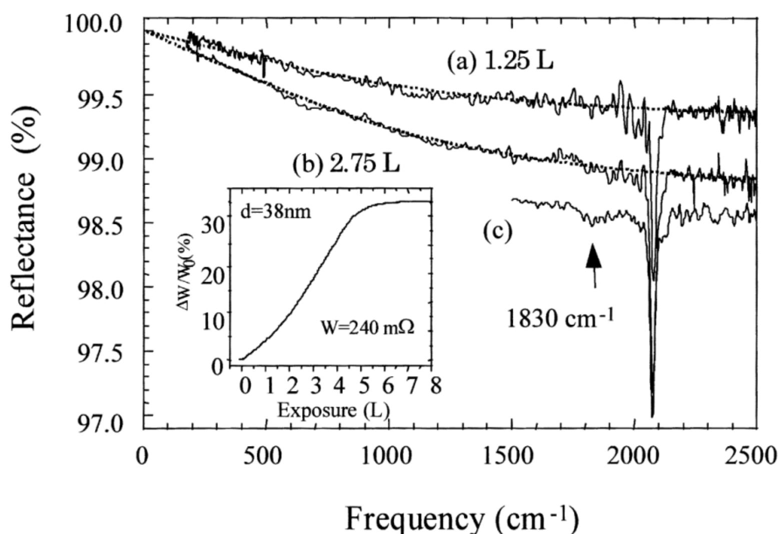

Figure 28. Infrared reflectance R spectra of a 67 nm Cu(111) film exposed to (a) 1.25 L and (b) 2.75 L of CO with vibration bands at ca 2080 cm^{-1} and 1830cm^{-1} (c) the spectrum taken with increased integration time to display the weak absorption band at 1830 cm^{-1} of CO adsorbed at bridge sites of the Cu(111) surface Inset: Increase of the resistance $\nabla W / W_0$ as function of CO exposure [3]

Resistance W means that Fermi electrons are not specular reflected at the surface, because of "friction" between the surface currents and adsorbed CO (see fig 27), thus creating a broad background of electron hole pairs. With decreasing frequency, the field of the excited electromagnetic surface waves extends further into the vacuum above the metal and become weaker at the surface. Therefore, the reflectance becomes 1 in the limit of decreasing frequency, as observed, see figure 28. The friction increases with the CO coverage and therefore the reflectivity at IR frequencies decreases by 1-2 % at the CO-stretch frequency at 2080 cm^{-1}. The resistance W increases with the CO coverage, see the inset in Fig. 28. The two CO stretch bands at 2080 and 1830cm^{-1} are explained by different adsorption sites of CO.

The expected fixed relation between ΔR and ΔW (see equation 10) was measured simultaneously, using an epitaxial Cu(111) film 67 nm thickness. The change of the film resistance was measured with the circuit shown in Fig 4. As expected, both quantities evolve in a similar way.

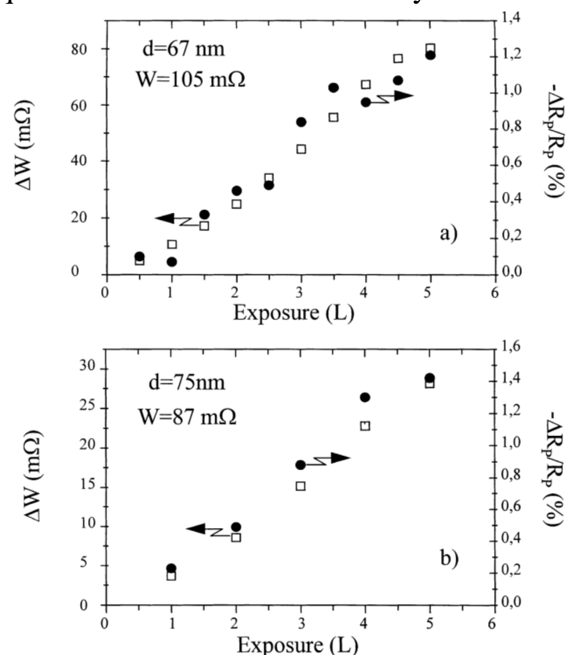

Figure 29. The resistance change ΔW (empty boxes) and reflectance changes (black dots) for 67nm and 75nm Cu(111) film as a function of CO exposure. The left scale ΔW refers to the change of the sheet resistance, the right scale refers to the

Copyright 2017 KEI Journals. All Rights Reserved

relative reflectance change for p-polarized polarization[18,3].

The relation between the changes of resistance and reflectivity is linear, see Fig. 29.

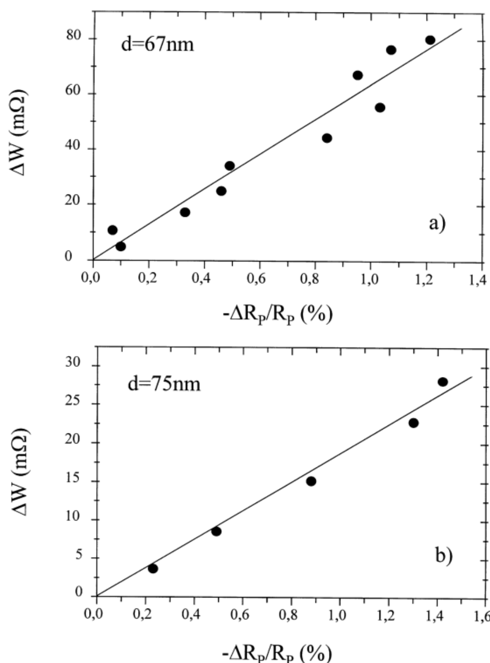

Figure 30. Relationship between the sheet resistance Delta W and the relative reflectance change delta Rp/Rp for (a) 67 and (b) 75 nm films of Cu(111) exposed to CO. The solid line is a linear fit.[18]

The resistance change by adsorbed ethene C_2H_4 is much weaker than for CO, see Figure 31.

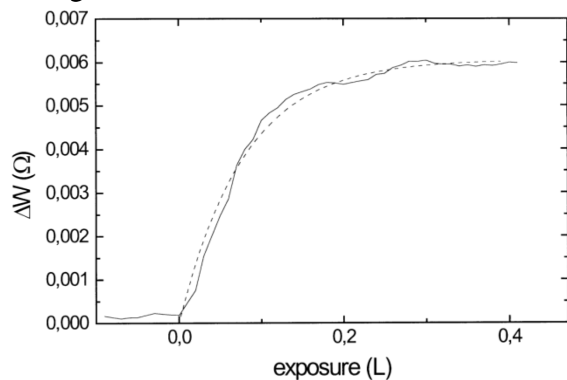

Figure 31. Absolute resistance change of a 33nm thick Cu(111) film due to C_2H_4 exposure [19].

The increase of resistance by exposure to C_2H_4 is very weak in comparison to CO (Figure 28). Accordingly the change of reflectivity is also very low, see Fig. 32.

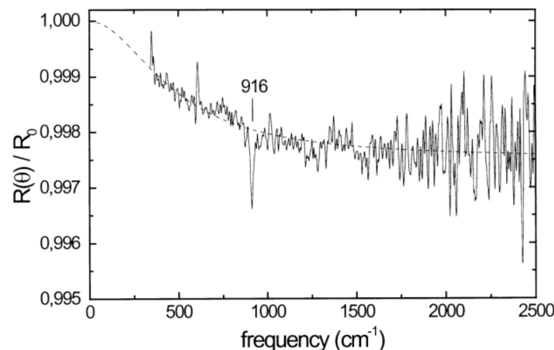

Figure 32. Reflectance spectrum of a 30nm thick Cu(111) film exposed to 0.16L C_2H_4, The asymptotic absorption is 0.0025[19].

Surprisingly, the coadsorption of CO and small quantities of C_2H_4 leads to a strong decrease of the reflectance (Fig. 33).

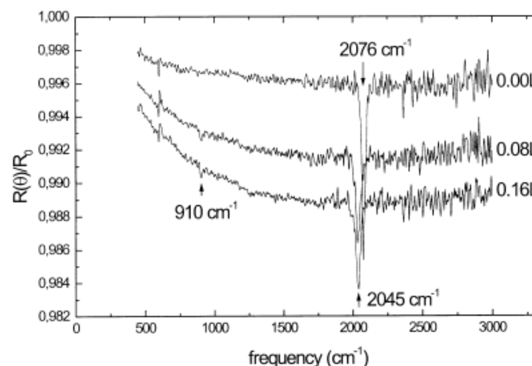

Figure 33. Change of reflectance of a 72nm thick copper film by 0.5L CO and additionally exposed to 0.08 L and 0.16 L C_2H_4 [19]

Copyright 2017 KEI Journals. All Rights Reserved

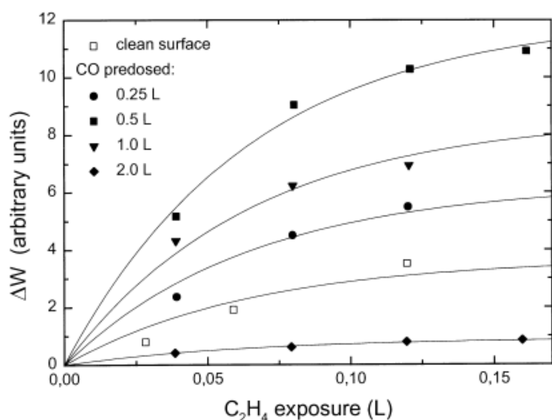

Figure 34. Resistance change ΔW of a 50nm clean and CO covered Cu(111) film due to additional exposure to C_2H_4 [19]

In Fig. 34, the resistance change ΔW at a precoverage of 2.0 L CO is very small , even smaller than under pure C_2H_4 exposure. This reflects full coverage of CO, leaving no surface sites for C_2H_4 adsorption.

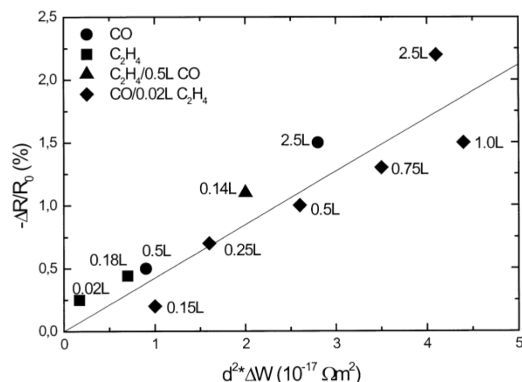

Figure 35. Relationship between the asymptotic limit of the reflectance decrease – ΔR /R in % and the resistivity change Delta W multiplied by the square of the film thickness for various adsorbates [19]

The interaction of CO and C_2H_4 may be understood with the help of Newns-Anderson model in Figure 36. The lowest unoccupied electronic states (dotted lines without interaction) will shift , caused by the CO-C_2H_4 interaction.

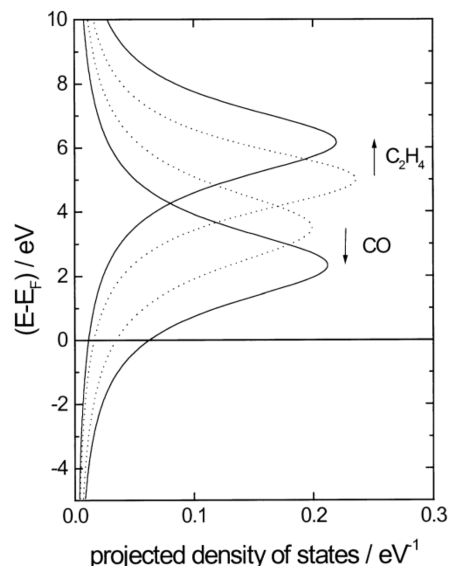

Figure 36. Electronic interaction of CO and C_2H_4 using the Newns-Anderson model. Dashed curves are the levels of the Pi star states without interaction, full curves with interaction. [19]

The energy of CO state is pushed to lower energy by the interaction with C_2H_4, see Figure 36, which leads to an increase of the surface resistance, as presented in figures 32 and 33.

0.1 monolayers of Cs on Cu(111) (see upper trace in Figure 37) do not change the reflectivity R, but the decrease of R after exposure 2.5L CO is doubled, see Fig. 37 .

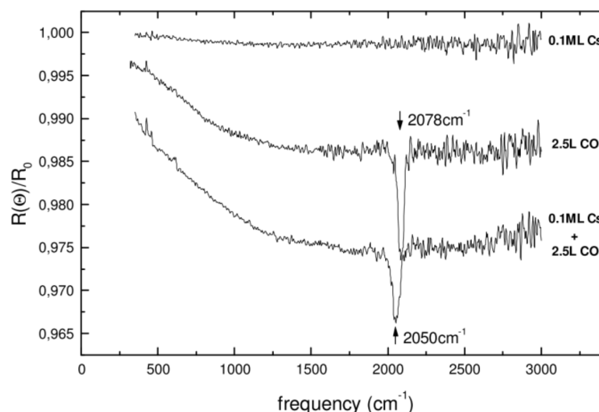

Figure 37. Change of the reflectance by pre-dosing the Cu(111) film by Cs. The frequency of the CO vibration is shifted. [3].

Copyright 2017 KEI Journals. All Rights Reserved

In Figure 37, 0.1 monolayers of Cs do not lead to a decrease in the reflectivity. But this weak Cs coverage diminishes the work function of the Cu film and the transient electron transfer from the Cu-Cs surface to the adsorbed CO molecules becomes more likely. This intensifies the decrease of reflectance R as shown in Fig. 37 [3].

The exception of a linear relationship between reflectance change and resistance change is verified by the results in Figure 38 for different adsorbates.

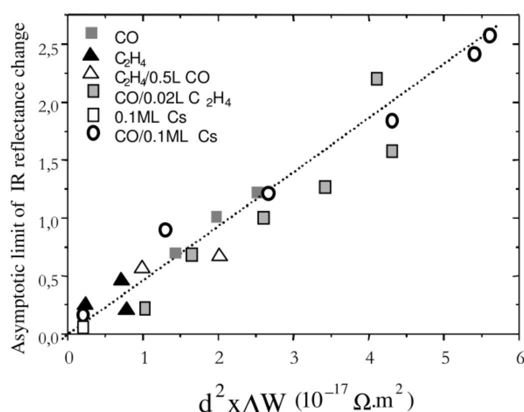

Figure 38. Relationship between the measured asymptotic limit of the reflectance decrease (-delta R/R) % and the resistivity change Delta W of Cu(111) thin films for various adsorbates (CO,C_2H_4,Cs) at different coverage. [3]

The linearity in Figure 38 is in line with the model involving the elastic scattering of the conduction electrons of the metallic substrate by the sliding adsorbate [3]

It was interesting to measure the change of the reflectance of CO adsorbed on a Cu (110) single crystal. Fig. 37 shows the surface of this crystal with the characteristic chains of Cu atoms in the (1,-1.0) direction [20]. The chains are parallel to the (1,-1,0) or (110) direction.

Experimentally, the crystal is rotated by 90° in the sample chamber in Figure 38.

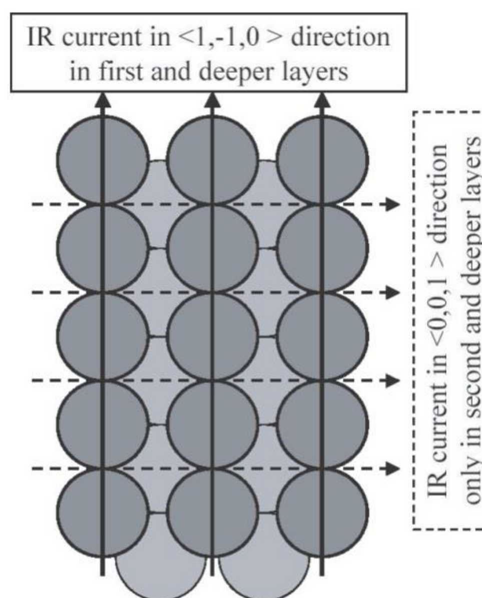

Figure 39. Atomic structure of the Cu(110) surface (1,-1,0)

The (110) crystal was rectangular with dimensions of 12.4 × 16.5 mm^2. The surface chains of Cu atoms are parallel to the (1,-1,0) direction. The crystal could not be rotated around its normal, but had to be inserted two times into the UHV vessel, with the (1, −1, 0) or the (001) direction in the plane of incidence. In both cases, the crystal was sputter annealed, the cleanliness checked by Auger electron spectroscopy (AES) and the orientation by low energy electron diffraction (LEED). The crystal was cooled to about 100 K before exposure to CO or C_2H_4. Two detectors were used, a boron-doped silicon bolometer (180–500 cm^{-1}) and a copper-doped germanium photoconductive detector (350–3000 cm^{-1}), both operated at 4.2 K.

The intensities caused by adsorbed CO and C_2H_4 display a strong inelastic background only when the polarisation (the direction of the electric vector of the incident radiation is parallel to the rows in (1,-1,0) direction, as shown in Figure 39.

Copyright 2017 KEI Journals. All Rights Reserved

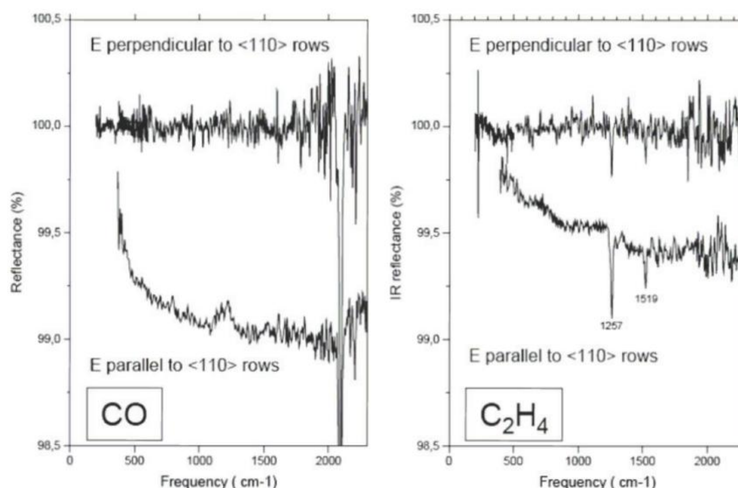

Figure 39. Reflectance spectra of CO and C_2H_4 adsorbed on the Cu(110) surface [20]

The spectra in Figure 39 show also the absorption band of the stretch vibration of CO at about 2100 cm^{-1} and the C-C stretch mode and CH_2 scissor modes at 1257 and 1519 cm^{-1}. For CO and E parallel to the <110> rows the reflectance increases like for CO adsorbed on a copper film, displayed in Figure 28.

12) Summary

Surface resistance (SR) is a concept, useful for many metal-adsorbate systems. SR has been measured in ultrahigh vacuum at low temperature for the first adsorbed layer of Xe and different molecules on Ag(111) films. The strong dependence of the surface resistance on the energy of the lowest unoccupied orbital supports the importance of transient electron-transfer between the silver film and the first adsorbed layer. Surface resistance of thin (111) silver electrodes in halide solutions display different potential of adsorption and desorption of halide ions, which is explained by the different size of the halide ions. SR of Ag(100) electrodes during adsorption was measured during underpotential deposition of Cu. Cd is detected for concentrations in the ppb range. Desorption of Au and recrystallisation of the first Au layer on a gold (111) electrode becomes evident SR. The predicted linear relation of SR and far infrared reflectivity was verified by IR radiation from a synchrotron. A strong background induced by adsorption of CO was explained, as well as the interaction of adsorbed CO and C_2H_4. Surface currents on a Cu(110) surface are only possible along the Cu rows, but not across the rows. Accordingly, the inelastic background and the IR bands of CO and C_2H_4 have only been observed for the IR polarization parallel to the Cu rows.

Acknowledgment

I thank Dieter Schumacher for introducing Matthias Hein and myself into the field of thin film resistance. I thank all my co-workers Hermann Grabhorn, Carsten Hanewinkel, Matthias Hein, Dirk Körwer and Philipp Lilie. We have profited very much from the theory of Bo N.J. Persson.

My special thanks go to Paul Dumas. He introduced Hein and myself to the IR equipment at the storage ring in Brookhaven. Without his help, many experiments would not have been possible.

Copyright 2017 KEI Journals. All Rights Reserved

Literature

1. Schumacher, D. *Surface Scattering Experiments with Conduction Electrons*. Springer: Berlin, 1992; Vol. 129, p 81.
2. Körwer, D.; Schumacher, D.; Otto, A. Resistance changes of thin electrodes of silver. *Berichte der Bunsengesellschaft, phys.chem.* **1991,** *95*.
3. Dumas, P.; Hein, M.; Otto, A.; Williams, G. P. Diffuse scattering of the conduction electrons of a metallic substrate by an adsorbate: an experimental study using synchrotron infrared radiation. . *SPIE Conference Proceedings* **1999**.
4. Lilie, P. Cyclovoltametrische und transiente Messung des Gleichstromwiderstandes während elektrochemischer Prozesse an Gold und Silberschichten. Inaugural-Dissertation, Heinrich-Heine-Universität, Düsseldorf, 2002.
5. Grabhorn, H.; Otto, A.; Schumacher, D. Variation of the DC-resistance of smooth and atomically rough silver films during exposure to C_2H_6 and C_2H_4 *Surface Science* **1992,** *264*.
6. Persson, B. N. J. Vibrational Dynamics at Siurfaces. *Journal of Electron Spectroscopy and Related Phenomena* **1990,** *54/55*.
7. Holzapfel, C.; Akemann, W.; Schumacher, D.; Otto, A. Variations of DC-Resistance and SERS Intensity During Exposure of Cold-Deposited Silver Films. *Surface Science* **1990,** *227* (1-2), 123-128.
8. Otto, A.; Frank, K. H.; Reihl, B. Inverse Photoemission of Pyridine on Silver(111). *Surface Science* **1985,** *163* (1), 140-152.
9. Bard, A. J.; Faulkner. *Electrochemical methods, Fundamentaly and Applications*. J,Wiley and sons: New York, 1980; p 718.
10. Winkes, H.; Schuhmacher, D.; Otto, A. Surface resistance measurements at the metal-electrolyte interface of Ag(100) and Ag(111) thin film electrodes. *Surface Science* **1998,** *400*.
11. Hanewinkel, C.; Otto, A.; Wandlowski, T. Change in surface resistance of an Ag(100) electrode by adsorbed bromide. *Surface Science* **1999,** *429*.
12. Winkes, H.; Schumacher, D.; Otto, A. Surface resistance measurements at the metal/electrolyte interface of Ag(100) and Ag(111) thin film electrodes. *Surface Science* **1998,** *400* (1-3).
13. Glück, O.; Schöning, M. J.; Lüth, H.; Otto, A.; Emons, H. Trace metal determination by dc resistance changes of microstructured thin gold film electrodes. *Electrochimica Acta* **1999,** *44*.
14. Michely, T.; Krug, J. *Islands,, Mounds and Atoms*. Springer: Berlin, 2003; p 313.
15. Budevski, E.; Staikov, G.; Lorennz, W. J. *Electrochemical Phase formation and growth*. VCH: Weinheim, New York, Basel, Cambridge,Tokyo, 1996; p 405.

Copyright 2017 KEI Journals. All Rights Reserved

16. Persson, B. N. J. Surface resistivity and vibrational damping in adsorbrd layers. *Phys.Rev.B* **1991,** *44*.

17. Persson, B. N. J.; Schumacher, D.; Otto, A. Surface Resistivity and Vibrational Damping in Adsorbed Layers. *Chemical Physics Letters* **1991,** *178* (2-3), 204-212.

18. Hein, M.; Dumas, P.; Otto, A.; Williams, G. P. Friction of conduction electrons with adsorbates - Simultaneous changes of DC resistance and broadband IR reflectance of thin Cu(111) films exposed to CO. *Surface Science* **1999,** *419* (2-3), 308-320.

19. Hein, M.; Dumas, P.; Otto, A.; Williams, G. P. CO interaction with co-adsorbed C_2H_4 on Cu(111) as revealed by friction with the conduction electrons. *Surface Science* **2000,** *465* (3), 249-258.

20. Otto, A.; Lilie, P.; Dumas, P.; Hirschmugl, C.; Pilling, M. W.; Williams;G.P. Anisotropic electric surface resistance ofCu(110). *New Journal of Physics* **2007,** *9*.

Copyright 2017 KEI Journals. All Rights Reserved